Study of the brain's dynamic functional connectivity with simultaneous fMRI-EEG: a network science approach

Francisca Ayres Ribeiro
francisca.ayres.ribeiro@tecnico.ulisboa.pt

Instituto Superior Técnico, Lisboa, Portugal

January 2021

Abstract

The brain's intrinsic organization into functional networks can be assessed using several imaging techniques, mainly functional magnetic resonance imaging (fMRI) and electroencephalography (EEG). While recent studies have suggested a link between the dynamic functional connectivity captured by these two modalities, the exact relationship between the fMRI and EEG functional networks spatiotemporal organization is still unclear. Furthermore, since these networks are spatially embedded, a question arises whether the topological features captured can be explained exclusively by the spatial constraints. We address these two questions by investigating the global and local structure of resting-state fMRI and EEG data, using a community and motif analysis, respectively, including a spatially informed null model. We show that even though fMRI and EEG functional connectomes are slightly linked, the two modalities essentially capture different information, with most but not all topology being explained by the spatial constraints.
Keywords: fMRI-EEG; network science; community analysis; motif analysis; spatial embedding

1. Introduction

Brain activity is believed to be organized into functional networks, reflecting the dynamic coupling between remote brain regions and the continuous exchange of information throughout the whole brain [1]. These networks can then be studied to characterize the spatiotemporal organization of the brain. Several studies have focused on spontaneous fluctuations that reflect coordinated activity in a context with no specific stimulus, also known as the resting-state [1–3]. Understanding the dynamic behaviour of these networks and their topology might be the key to increase the understanding of brain's complex activity and, possibly, provide biomarkers for neurological and psychiatric diseases [4, 5].

These functional networks can be defined using different imaging techniques, such as functional Magnetic Resonance Imaging (fMRI) and electroencephalography (EEG), that allow the characterization of time-varying activity in the whole brain. However, these techniques have distinct temporal and spatial resolution and are sensitive to different physiological changes associated with neuronal activity [6]. Even though both reveal the brain's dynamic behaviour, it is still not entirely known how the two measures are correlated with each other, i.e., what is the relationship between the hemodynamic response and electric activity, and whether they capture the same information or not [7].

In recent years, several studies have analyzed functional connectivity by combining simultaneously acquired EEG-fMRI recordings with the objective of establishing a correlation between the two and also to take advantage of their complementarity [7–9]. Moreover, this type of analysis can provide richer characterization of the spatiotemporal organization of the brain activity. Nonetheless, no study to date has performed a comparative analysis between these two modalities functional networks by investigating their topology over time.

The analysis of these functional networks can be done considering a graph theory framework that allows the brain functional systems to be modeled as complex networks [4]. In this context, the functional networks and their dynamic topology can be studied by analyzing their global properties, like the community structure [10–12] or by exploring how these networks are organized on a local perspective, using motif analysis [13, 14]. Furthermore, since these networks are spatially embedded, the question arises whether the topological features captured can be explained by the impositions determined by the brain's underlying structure [15] or if there is still some functional synchronization deviating from these proximity constraints. Some studies have already explored this space effect in structural networks [15, 16] and, more recently, in the community structure of functional networks, considering only long-distance connections [17].

Therefore, this thesis intends to fill the gap in the present literature by performing a comparative network analysis with fMRI and EEG functional connectivity data, both on a macro- and meso-scale, by means of a community and a motif analysis, respectively. For that, several established approaches were used, such as the Louvain algorithm [18] for the extraction of modules of coordinated activity, as well as its multiplex version [19], here applied to find partitions combining fMRI and EEG for the first time, and also the g-tries data structure [20] to ef-

ficiently count occurrences of motifs in these functional networks. Also, with hopes of exploring the influence of space in the global and local topology, it was investigated the functional networks topology beyond these spatial constraints. Hence, new approaches were applied, such as a modified version of the Louvain algorithm [21], that includes a degree constrained spatial null model in the modularity definition, and also a motif analysis where the subgraphs are tested against this spatial null model.

2. Background and Related Work

2.1. fMRI-EEG

2.1.1 FMRI and Functional Connectivity

Functional Magnetic Resonance Imaging (fMRI) is one of the most widely used imaging techniques, since it allows a noninvasive whole-brain analysis. It measures brain activity based on changes in the blood flow consisting in a blood-oxygen-level-dependent (BOLD) signal, tightly correlated with neuronal activity [6]. These changes, however, come slow and with a significant delay, which impacts temporal resolution [22]. FMRI is typically used for the mapping of brain regions regarding their activity over time due to its high spatial resolution, but it can also unravel how these neural systems are functionally coupled together. [23]

Functional connectivity measures the similarity between the activity of anatomically separated brain regions, reflecting the level of functional interaction between them [1]. It can be examined through the study of spontaneous changes in the BOLD signal over time, using resting-state fMRI. This dynamic behaviour, denoted as dynamic functional connectivity (dFC), is typically characterized using a sliding window approach. This consists in segmenting the BOLD time-series from the brain regions (or voxels) into a set of temporal windows, within each the pairwise correlation is examined [5]. However, this compromises the temporal resolution by averaging the correlation over the time frame [24].

To not lose temporal resolution, dFC can be measured instantaneously using phase coherence (PC). The idea behind this approach is to compare two brain regions' signals, regarding the instantaneous phase information of the time-series [24], and use their degree of synchronization as a measure of connectivity. Assuming a narrow-band signal, the instantaneous phase can be obtained using the Hilbert transform (see [24] for more details) and then, the phase coherence between two brain regions corresponds to the cosine of the difference of their instantaneous phases. Computing for all brain regions will result in a phase coherence matrix for each time point [25].

2.1.2 EEG and Functional Connectivity

Electroencephalography (EEG) allows the direct measurement of transient brain electrical dipoles generated by neuronal activity [6]. With the use of scalp electrodes, this constitutes a non-invasive method to record electrical activity, with high temporal precision [26], which makes it appealing for the study of resting-state dFC. EEG recordings are conventionally decomposed into five main frequency components: delta (1-4 Hz); theta (4-8 Hz); alpha (8-12 Hz); beta (12-30 Hz); gamma ($>$ 30 Hz). Each frequency band is associated with different functions and origins, with low-frequency oscillations being usually associated to coordinated activity of large-scale neuronal networks, whereas high-frequency oscillations mostly reflect synchronization between nearby cortical regions [27].

Functional connectivity can be characterized using a variety of connectivity metrics, mostly computed using the EEG signals in the frequency domain, which characterizes an estimate of amplitude and phase of the neural oscillations captured across time [28]. To represent these signals this domain, a Fourier decomposition can be applied [29].

However, most connectivity metrics are susceptible to the volume conduction effect and can yield spurious connectivity. This because there is an inevitable mixing of overlapping signals arising from distinct brain sources at the EEG electrodes, due to the conductivity of the electrical signals spreading from the tissues to the scalp [30, 31]. To retrieve true neuronal interaction, it is necessary to use metrics robust to volume conduction, by ignoring zero-lag synchronizations between signals arising from the same source [32]. This is the case for the imaginary part of coherency. This metric isolates the part of coherency that reflects the actual interaction between two signals, removing the amplitude components (corresponding to contributions along the real axis) susceptible to volume conduction [32].

Another possibility to reduce the effects of volume conduction is by establishing functional connectivity directly at the source level [33]. The transition from the electrodes to the source space can be done through source reconstruction, i.e., the localization of the underlying sources and reconstruction of the associated time series [34]. This involves solving the inverse problem by means of regularization strategies, which typically consist in weighted minimization approaches.

2.1.3 Multimodal fMRI-EEG

Both fMRI and EEG allow the study of whole-brain dFC by probing neuronal activity through distinct biophysical processes and with different spatial and temporal resolutions. As such, there is an increase interest in integrating both modalities and take advantage of their complementarity [35], with the objective of unraveling the neuronal coupling of EEG and fMRI. This can be done with simultaneous acquisitions, allowing temporal equivalence and thus establishing a parallel between both modalities' dFC [7].

Nonetheless, this gives rise to many artifacts that can completely compromise the signal due to electromagnetic perturbations originated from both systems and their interaction [36]. Therefore, it is necessary to apply denoising techniques and removal of artifacts that appear specifically in this multimodal acquisition.

To analyze simultaneous fMRI-EEG data and compare their dFC, it is convenient to define a spatial mapping between the two signals, i.e., an equivalence between the brain regions defined for fMRI and the sources of the EEG signals detected by the electrodes, which can be

achieved through source reconstruction.

2.2. Brain Complex Networks

The brain's functional systems can be modeled as complex networks through the measurement of pairwise interactions between brain regions. Graph theory based analysis has emerged as a powerful new tool to analyze brain imaging data and capture the dynamic of functional networks [4]. It provides a theoretical framework in which the networks' topology can be investigated, unraveling information about local and global organization, possibly exposing otherwise hidden phenomena [1].

A graph representation of a network is given by the tuple $G = (V, E)$, where V is the set of nodes or vertices, corresponding in this context to the brain regions, and $E \subseteq V \times V$ the set of links or edges that compose the network, reflecting the functional synchronizations. This is often represented by an adjacency matrix, whose elements different than 0 indicate the presence of connections between each pair of nodes. Therefore, functional connectivity can be assessed constructing graph representations from the connectivity matrices reflecting the correlation between brain regions. In order to retain significant interactions and exclude spurious connections and noise, these matrices are usually thresholded, which can be done with a cut-off threshold or using a proportional one that keeps a certain percentage of the top connections [33].

From this graphical model, it is possible to assess parameters of interest, such as node degree, clustering coefficient and average path length. The full definition and how to compute these metrics is reviewed in [37]. But making a general overview, the node degree corresponds to the number of connections linking a node to the rest of the network, being possible to establish a degree distribution, which can reveal the topology of the network. The clustering coefficient reflects the network's tendency to form topologically local circuits, this way measuring information segregation, and it can be regarded as a measure of local efficiency. In turn, the average path length represents the global efficiency of a network, as it measures how close a node is, on average, to every other node of the network.

2.2.1 Null Models

When analyzing functional networks and their topology, independently of the metrics being investigated, it is important to guarantee that the results are representative. This can be achieved by comparing them with the ones extracted from a suitable null model. This corresponds to a randomized version of the original network, still preserving some of its properties, except the ones being tested. Consequently, for a meaningful conclusion to be drawn about the network's organization, there needs to exist a significant difference between the null model and the original network observations, i.e., they must deviate from what would be expected by chance [37]. Typically, this assessment is done by means of the computation of a z-score or p-value, from statistical testing. The most commonly used null model when analyzing brain networks is the rewiring null model, which can be generated by the Maslov-Sneppen rewiring algorithm [38]. It preserves the network size, density and degree distribution, which will naturally affect the networks topology. However, other features can be contemplated in a random network to more accurately reproduce the topology observed in the brain. For instance, it is often overlooked that these networks are physically constrained by the anatomical space and also by the cost of maintaining connections between different regions, which gives primacy to local connectivity and results in few long-range connections [16]. To overcome this limitation, these physical distances can be included, creating spatial constraints that will guarantee a more realistic null model [37]. That is the case of the spatial null model proposed in [21], a gravity-based model that contemplates the proximity effect and also preserves the degree distribution of the original network. This model assumes that the probability of a connection between two regions is proportional to their intrinsic strength and decays with distance:

$$P_{ij} \sim n_i n_j f(d_{ij}), \tag{1}$$

where n_i is the intrinsic strength of node i, $f(d_{ij})$ corresponds to an estimated deterrence function that describes the effect of distance d_{ij}.

2.2.2 Community Analysis

Functional connectivity can be analyzed to identify modules or patterns reflecting coherent activity between different brain regions. Therefore, it is possible to further analyze the topology of these brain networks to unravel these structures, both on a macro- and meso-scale.

On a macro-scale, the presence of partitions in the network can be investigated, reflecting its global structure and organization into densely connected clusters with relatively few connections between them. This analysis can reveal groups of brain regions with coordinated activity by means of community finding algorithms, typically based on modularity maximization, where the Louvain algorithm is the commonly used in brain networks [11, 12, 39, 40].

However, since the brain networks are physically constrained, one might question if the modular organization present is solely the result of the effects of space. Cazabet et al. [21] proposed a modification of the Louvain algorithm, to include the degree constrained spatial null model (described in section 2.2.1) in the modularity definition. This way, it is possible to regress out the spatial constraints and find if long-range functional connectivity contributes to global structure of the functional networks.

Even though such method has not been applied yet to functional networks, some studies have suggested that, despite the neural systems tendency to show an optimal spatial arrangement by minimizing the wiring and distance, this is not the only factor for the configuration observed [41]. Additionally, a recent study has shown that, even when removing the short-distance connections, there is still a community structure present in the functional networks [17].

Additionally, to characterize the dFC combining both fMRI and EEG data, a multilayer framework can be used, where each layer corresponds to each imaging technique.

As such, an extension of the Louvain algorithm to a multilayer context [19] can then be applied to retrieve the community structure arising when combining both modalities.

2.2.3 Motif Analysis

To identify patterns of synchronized activity or topological features on a meso-scale, the existence and count of overabundant small building blocks in the network can be explored. This reveals additional information about local structure and can be used as networks fingerprints or signatures [42]. These network motifs are small induced subgraphs that appear in a larger network at a higher or lower frequency than it would be expected, that is, are statistically significant when compared to an adequate null model. These motifs can then be used to find differences in brain functionality between groups, equivalence between networks due to similar local structure or simply to analyze functional connectivity coupling between a few brain regions with respect to some baseline [43, 44]. Therefore, they have the power to characterize and discriminate different networks.

One efficient way to store and enumerate them is to resort to g-tries data structure, proposed by Ribeiro and Silva [45], suited for enumerating many small graphs up until five nodes and with different shapes in large networks [20]. This is possible as this tree-like structure stores all common subtopologies between subgraphs in a compact way, avoiding redundancies and guaranteeing that each occurrence is only counted once.

3. Data Representation

3.1. Data Acquisition and Preprocessing

The dataset used in this work consists in simultaneous fMRI-EEG recordings acquired during rest in the scope of a previous project [46], using a 7T MRI scanner along with a 64-channel EEG system, involving 9 healthy subjects. The data preprocessing and brain segmentation were made according to [47]. As such, the BOLD time-series were bandpass-filtered at 0.009-0.08Hz, while the EEG signals were filtering at 0.3-70 Hz and segmented as a multiple of the Repetition Time (TR) of the fMRI acquisition (TR 1s).

3.2. Construction of Functional Networks

With the objective of the analysis of and comparison between the fMRI and EEG functional networks' topology on a meso- and macro-scale, a graph representation was used. The nodes were set as the regions of interest defined by the Desikan(-Killiany) atlas [48], equivalent for both modalities. This spatial alignment is guaranteed by a source reconstruction procedure, using the Tikhonov-regularized minimum norm [49], as described in [47]. The edges, on the other hand, were defined by the functional connectivity matrices obtained for each time point using phase coherence and imaginary part of coherency, respectively. This was estimated using an adaptation of Cabral et al.'s implementation (`https://github.com/juanitacabral/LEiDA`) [25] and using the Brainstorm function *bst_cohn.m* (according to the Brainstorm 2018 implementation `http://neuroimage.usc.edu/brainstorm`, 'icohere' measure) as described in [47], respectively. Furthermore, the imaginary part of coherency estimation was averaged for the 5 canonical frequency bands: delta δ (1-4 Hz), theta θ (4-8 Hz), alpha (8-12 Hz), beta β (12-30 Hz), gamma γ (30-60 Hz).

To guarantee temporal equivalence between fMRI and EEG functional networks, some connectivity matrices fMRI were removed for the fMRI, corresponding to the time points excluded from the EEG data due to excessive motion. Furthermore, as the BOLD time-series have an intrinsic delay with respect to the EEG data, due to the different nature of the two signals, this temporal shift was estimated using a resting-state hemodynamic response function (HRF) deconvolution toolbox (`https://github.com/compneuro-da/rsHRF`), corresponding to 3-4 seconds, depending on the subject.

Finally, to remove any spurious connectivity arising from noise or artifacts typical on this type of dataset, these functional networks were thresholded while guaranteeing that the giant component was still present for most time points. For that, a data-driven percolation approach was used to select a proportional threshold for fMRI and each EEG frequency band, that is, the percentage of edges necessary to avoid the collapse of the giant component. The resulting threshold values are 11%, 7.5%, 6.6%, 7.0%, 6.1%, 7.0% and 6.5% for fMRI and EEG delta, theta, alpha, beta and gamma frequency bands, respectively.

4. Methods

4.1. Community Analysis

A community analysis was performed to characterize both fMRI and EEG functional networks on a macro-scale, to explore their potential correlation over time and also to investigate the possible influence of the proximity constraints in the modular structure captured.

4.1.1 Null Model Comparison Analysis

First, the global topology of these functional networks was analyzed over time in comparison to a rewiring null model, using three metrics: clustering coefficient, average path length and modularity, computed using the Louvain algorithm (using NetworkX's functions). Then, the time points for which the functional networks deviate from the random case were selected. This statistical testing was done for all three metrics by generating 100 surrogates for each corresponding network and computing the resulting p-value, selecting the time instances with $p < 0.05$. The time points selected for each of the three metrics were then intersected, for each modality. Lastly, a unique set of time points was obtained for both fMRI and EEG networks by choosing only the common selected ones, for each frequency band independently. Since the topology observed may be due to spatial constraints, this same analysis was performed with respect to a degree constrained spatial null model [21]. As such, it was selected a second set of time points deviating from what is expected by the influence of space.

4.1.2 Louvain algorithm

With the objective of identifying modules of synchronized activity, potentially similar between modalities, the com-

munity structure of these functional networks was analyzed. This was done for each set of selected time points obtained previously, with respect to the rewiring null model, using the Louvain algorithm (with NetworkX's community package). Following this, the median modularity was estimated, for both fMRI and EEG frequency bands. To explore the potential correlation between the two modalities regarding to the modular structure captured by both functional networks, the communities extracted were compared for all selected time points, using the Normalized Mutual Information (NMI) and Jaccard Index metrics.

4.1.3 Modified Louvain algorithm

Considering the influence of the spatial constraints in the functional networks topology, it was desirable to check if some modular configuration present in these functional networks emerges from functional necessity and not just as a consequence of space proximity. With this objective, the community structure of these functional networks beyond these spatial constraints was investigated. This was done for all selected time points obtained previously with respect to the degree constrained spatial null model, using the modified Louvain algorithm (*spaceCorrectedLouvainDC* toolbox) [21]. Then, the median modularity was estimated, for both fMRI and EEG frequency bands. Additionally, the communities extracted with and without the spatial influence were compared over time using the NMI metric, to investigate their difference. Finally, the communities extracted while regressing out the influence of space were compared for all time points, again using the NMI and Jaccard Index metrics. This was done to distinguish and quantify the influence of the spatial constraints in correlating the two modalities and verify if there is a correlation beyond that, reflecting the underlying synchronous activity captured by the two.

4.1.4 Multiplex Louvain algorithm

To investigate if combining fMRI and EEG information can lead to new and improved results, a multilayer version of the Louvain algorithm [19] was used to extract communities common to both modalities for all time points selected using the rewiring null model. This algorithm was applied as a multiplex case, i.e., when all the layers share the same node set since there is a spatial equivalence betwen fMRI and EEG networks, using i-graph's louvain package *find_partition* function. Following this, the median improved modularity was estimated, for both fMRI and EEG frequency bands. In parallel, the median modularity associated to these communities when isolating the two layers was obtained to check if different partitions were obtained for each modality in comparison to the previous optimized ones (in section 4.1.2). Additionally, these values were compared with the ones obtained for the degree constrained spatial null model of both modalities.

4.2. Motif Analysis

A motif counting analysis was performed to characterize both fMRI and EEG functional networks on a mesoscale, to explore their potential correlation over time and also to investigate the influence of the proximity constraints, imposed by the spatial embedding in the local structure captured for the two modalities. This analysis was done using the g-tries algorithm proposed by Ribeiro et al. (available in `https://www.dcc.fc.up.pt/gtries/#manual`) [20], considering undirected subgraphs with 3, 4 and 5 nodes, which correspond to 2, 6 and 21 different motif classes, respectively. It was considered that these subgraphs were enough to characterize and distinguish the different functional networks, with 5 nodes subgraphs leading to a finer analysis.

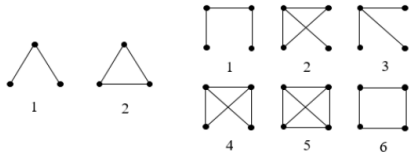

Figure 1: The 2 and 6 possible subgraphs of size 3 and 4, respectively

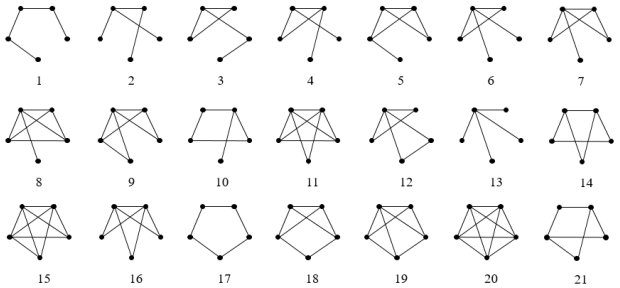

Figure 2: The 21 possible subgraphs of size 5

4.2.1 Motif Analysis with Rewiring Null model

To identify subgraphs that are over- or under-expressed against a rewiring null model, the g-tries algorithm was used directly, retrieving the number of occurrences and z-score for each subgraph. Then, to discriminate the most significant ones, the percentage of time points for which each motif class appeared on the significance top was computed, that is, considering all the time points where that specific motif was one of the most over- or under-represented (z-score > 2 and < 2, respectively), for fMRI and EEG functional networks independently. Moreover, to analyze the motif diversity across time, the variation of the total number of motif classes was obtained, for each modality separately. Finally, to study the correlation between them regarding the motifs extracted and thus between the local functional organization captured by each imaging technique, the network fingerprints, defining a motif profile for each functional network, were computed and compared for all time points, using the cosine distance metric. These network fingerprints were defined by the number of occurrences of each motif class, normalized by the total of all motifs, for each time point.

4.2.2 Motif Analysis with Degree Constrained Spatial Null model

To verify the impact of the spatial influence in the motifs present in both functional networks and to investigate which still occur beyond these constraints, the subgraphs obtained using the g-tries algorithm were tested against

the ones retrieved from the degree constrained spatial null model. The following analysis was similar to the one described in section 4.2.1.

5. Results and Discussion

5.1. Community Analysis

5.1.1 Null Model Comparison Analysis

The overall results of the null model comparison for both fMRI and EEG functional networks, using the rewiring and spatial null model are reported hereafter. Figures 3 and 4 illustrate the temporal variation for the modularity values, chosen between the three metrics for representation as they showed similar behaviour, in comparison to each null model respectively. Table 1 summarizes the percentage of time points deviating from these null models, averaging for all subjects.

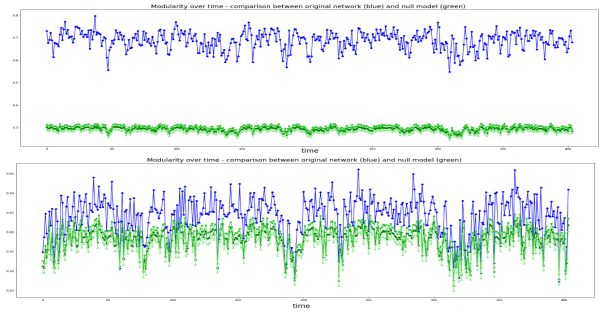

Figure 3: Temporal variation of modularity (blue) for fMRI and EEG beta, respectively, in comparison to the rewiring null model (green).

From these results, it is noticeable an oscillation over time, for both modalities, which is not surprising considering that brain functional connectivity tends to oscillate between segregated and integrated states [11,33,39,50]. Besides this, there is a big difference between the fMRI and EEG functional networks, as the first one appears to possess a much clustered structure than the second one. As such, the resulting time points obtained from the intersection between the two modalities' selection were almost entirely the same as for the EEG.

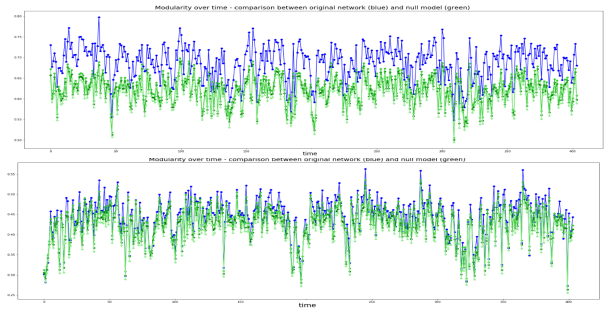

Figure 4: Temporal variation of modularity (blue) for fMRI and EEG beta, respectively, in comparison to the degree constrained spatial spatial null model (green).

Furthermore, the degree constrained spatial null model presents a somewhat clustered topology, constituting an important contribution for the structure observed. This is not surprising since it has been reported a general tendency for the clusters in functional networks to be composed by regions that are near one another in the physical space [51]. In particular, the spatial null model appears to be almost identical to the EEG functional networks, suggesting that the little topology detected for this modality might be a result of the spatial constraints imposed in these functional networks. This means that the EEG seems to be more susceptible to these proximity constraints than the fMRI, which might result from the lower spatial resolution intrinsic to this imaging technique. Nevertheless, it resulted in a low percentage of time points selected for both modalities, where the delta band seems to deviate the most from the spatial null model, possibly due to its ability to capture synchronized oscillations between brain regions at a longer distance than higher frequencies [27, 52].

Table 1: Percentage of time points for which both modalities functional networks reflect a clustered structure in comparison to both rewiring and degree constrained spatial null model - for each frequency band, averaged for all subject (and with corresponding standard deviation (std).

fMRI-EEG pair	delta	theta	alpha	beta	gamma
Rewiring					
average (%)	60.6	56.8	59.1	59.5	65.3
std	± 6.5	± 5.3	± 5.3	± 7.1	± 11.4
Spatial					
average (%)	12.9	7.0	9.1	7.2	9.9
std	± 3.5	± 2.0	± 1.2	± 1.9	± 4.0

5.2. Louvain algorithm

The overall results of the community analysis with the Louvain algorithm, using the time points selected with the rewiring null are reported hereafter, for both fMRI and EEG functional networks. Table 2 summarizes the median modularity obtained for each modality, averaging for all subjects. Figure 5 shows the correlation over time between the two modalities, for arbitrary frequency band and subject. Table 3 represents the average NMI and Jaccard Index value obtained from the comparison of the community structure of both functional networks.

Table 2: Median modularity values associated to the communities extracted from fMRI and EEG frequency bands over time using the Louvain algorithm, averaged for all subjects (with associated standard deviation (std)). These modularity values were computed considering each set of selected time points, using the rewiring null model, for every pair fMRI-EEG frequency band.

fMRI-EEG pair	delta	theta	alpha	beta	gamma
fMRI					
average	0.700	0.700	0.697	0.699	0.699
std	± 0.004	± 0.005	± 0.005	± 0.004	± 0.015
EEG					
average	0.455	0.466	0.447	0.465	0.428
std	± 0.004	± 0.002	± 0.003	± 0.010	± 0.015

In line with the previous observations, the fMRI functional networks show a much more modular configuration than the EEG, which is in accordance with previous dFC studies suggesting a more moderate modularity for the EEG networks in comparison to the high value found for the fMRI case [53]. Moreover, the less modular topology retrieved for the EEG might be due to a worse quality of the data collected, as it is more affected by artifacts [54–56] or to a lack of sensibility of the imaging technique to capture the topology of the underlying functional

networks [30, 57], because of the difficulty in performing an accurate source reconstruction, specially for resting-state data [58].

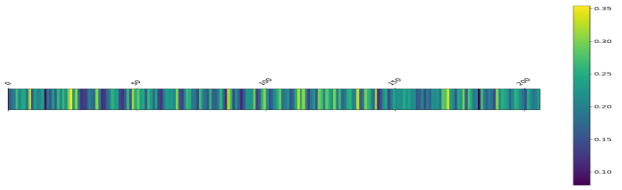

Figure 5: NMI coloured array regarding the comparison of the communities obtained over time with the Louvain algorithm, between fMRI and EEG alpha band, for subject 8.

Table 3: NMI and Jaccard Index values (and associated standard deviation (std)) obtained from the comparison of fMRI and EEG frequency bands community structure obtained using the Louvain algorithm, averaged for all subjects.

fMRI-EEG	delta	theta	alpha	beta	gamma
NMI					
average	0.247	0.265	0.262	0.287	0.273
std	± 0.048	± 0.048	± 0.053	± 0.049	± 0.053
Jaccard					
average	0.183	0.185	0.184	0.185	0.186
std	± 0.026	± 0.027	± 0.027	± 0.027	± 0.028

There is indeed a moderate correlation between the topology captured by the two modalities, as it can be observed from the NMI and Jaccard Index results, which are in line with previous reports for the comparison of fMRI and EEG static connectomes [47] using the same dataset. Also, it is also in accordance to studies examining dFC with both modalities, reporting a link between the two [9, 52, 59, 60]. Nevertheless, this correlation is not particularly high, which might be due to the lack of modular topology in the case of EEG, as discussed. But it might also be that this modality captures different interactions, resulting in a more integrated topology instead of segregated one, as found for the fMRI networks. In fact, it has been shown in [61] that EEG functional connectivity clusters into groups of brain regions in a different way than the fMRI functional connectivity, and that these clusters appear to be extended in space, with lower connectivity within modules than between them. Moreover, from the coloured arrays, it is noticeable an oscillation in similarity over time, which was found to be specific to each frequency band. This not surprising considering past studies have reported a different contribution of each EEG frequency band to the BOLD connectivity dynamics [8, 52, 62], varying across space [63], with a more local topology captured for higher frequency bands such as the gamma band and a more global connectivity for lower ones, like the delta band [27, 53, 59, 64].

5.3. Modified Louvain algorithm

The overall results of the community analysis with the modified Louvain algorithm, using the time points selected with the spatial null are reported hereafter, for both fMRI and EEG functional networks, to further analyze the spatiotemporal organization of these networks beyond spatial constraints. Table 4 summarizes the median modularity obtained for each modality, averaging for all subjects. Figure 6 shows the comparison between the communities obtained over time with and without the spatial constraints, while figure and 7 shows the correlation over time between the two modalities still arising beyond the influence of space, for arbitrary frequency band and subject. Table 5 represents the average NMI value obtained from the comparison of the community structure of both functional networks.

Table 4: Median modularity values associated to the communities extracted from fMRI and EEG frequency bands over time using the modified Louvain algorithm, averaged for all subjects (with associated standard deviation (std)). These modularity values were computed considering each set of selected time points, using the degree constrained spatial null model, for every pair fMRI-EEG frequency band.

fMRI-EEG pair	delta	theta	alpha	beta	gamma
fMRI					
average	0.072	0.071	0.073	0.072	0.071
std	± 0.002	± 0.005	± 0.003	± 0.004	± 0.003
EEG					
average	0.036	0.034	0.034	0.032	0.033
std	± 0.003	± 0.002	± 0.001	± 0.002	± 0.002

Even though the spatial constraints seem to explain the majority of the topology observed in fMRI and EEG functional networks, as it was observed in the null model comparison analysis, it was still possible to retrieve some community structure beyond these expectations. Also, despite the resulting modularity values being quite low, they are associated to functional networks deviating from a random configuration, therefore making the corresponding communities statistically significant.

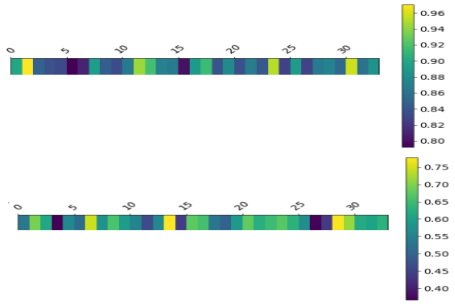

Figure 6: NMI coloured arrays regarding the comparison of the communities obtained over time with and without the spatial constraints, between fMRI and EEG theta band, respectively, for subject 7.

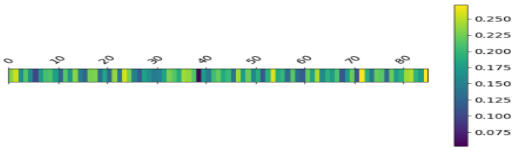

Figure 7: NMI coloured array regarding the comparison of the communities obtained over time with the modified Louvain algorithm, between fMRI and EEG delta band, for subject 2.

When comparing the communities obtained with the regular and modified version of the Louvain algorithm, it is possible to notice that there is an overall high similarity but not a complete match. Suggesting the existence

of relevant spatial patterns that arise out of functional necessity and not just as a consequence of space, even if not at a major extent. Furthermore, it is important to note that these similarity values are lower for the EEG implying that, even though there is not as distinct modular structure as for the fMRI, the spatial effects seem to have a higher impact in EEG networks topology.

Comparing fMRI and EEG community structure beyond the spatial constraints, it was obtained lower similarity overall than when using the regular Louvain algorithm. These results point out the possibility of having a portion of the correlation between the two guaranteed by the underlying spatial embedding. Even so, it was still possible to retrieve some correlation beyond the spatial constraints, which further supports the link between the fMRI and EEG dynamic functional connectivity. Nonetheless, it is important to take into consideration that this analysis is done only for the time points deviating from the spatial null model (around 9%).

Table 5: NMI and Jaccard Index values (and associated standard deviation (std)) obtained from the comparison of fMRI and EEG frequency bands community structure obtained using the modified Louvain algorithm, averaged for all subjects.

fMRI-EEG	delta	theta	alpha	beta	gamma
NMI					
average	0.182	0.199	0.193	0.211	0.207
std	± 0.052	± 0.052	± 0.057	± 0.060	± 0.061
Jaccard					
average	0.187	0.187	0.182	0.186	0.186
std	± 0.040	± 0.040	± 0.035	± 0.042	± 0.040

5.4. Multiplex Louvain algorithm

Since it was not retrieved a total match between the topology captured by two modalities on a global scale, despite the moderate correlation found, one can speculate that these complementary imaging techniques capture different information regarding the underlying neuronal activity and its functional organization. The improved median modularity resulting from the multiplex Louvain algorithm analysis are reported in table 6, as well as the individual values obtained for each of the two modalities.

Table 6: Median modularity values associated to the common communities extracted from both fMRI and EEG frequency bands over time using the multiplex Louvain algorithm, averaged for all subjects (with associated standard deviation (std)). These modularity values were computed considering each set of selected time points, using the rewiring null model, for every pair fMRI-EEG frequency band.

fMRI-EEG pair	delta	theta	alpha	beta	gamma
multiplex fMRI-EEG					
average	0.747	0.752	0.748	0.755	0.751
std	± 0.004	± 0.004	± 0.005	± 0.005	± 0.005
individual fMRI					
average	0619	0.591	0.603	0.571	0.615
std	± 0.011	± 0.010	± 0.009	± 0.009	± 0.007
individual EEG					
average	0.091	0.123	0.105	0.148	0.102
std	± 0.009	± 0.009	± 0.005	± 0.011	± 0.014

One can immediately notice that the individual values obtained here are lower than the single-layer ones reported before in section 5.2. Meaning that the multilayer approach finds clusters common to both modalities that were not found previously, since these partitions possessed too low modularity to be selected by the community detection procedure. As such, this suggests that using the two modalities together leads to interesting communities that would not be found if looking at each functional network individually. These findings are in line with two previous studies that performed a joint-analysis of these modalities, by means of a hybrid independent component analysis [53] and by building a multimodal graph, joining the fMRI and EEG nodes into a single network [8], to identify new connectivity structure. Furthermore, the modularity found was statistically significant in comparison to a multiplex spatial null model for most time points, implying that it is not just the spatial embedding that leads to the common partitions selected.

5.5. Motif Analysis

5.5.1 Motif Analysis with Rewiring Null Model

The overall results of the motifs analysis of both fMRI and EEG functional networks, with respect to the rewiring null model are reported hereafter. Table 7 summarizes the most recurrently over- and under-represented motifs order according to the percentage of time points they appear in. Figure 8 illustrates the temporal variation of the number of motifs over- and under-expressed in these functional networks. Figure 9 shows the correlation between fMRI and EEG network fingerprints over time. The results represented here concern 5 node motifs, since it led to a finer analysis than with 3 and 4 nodes.

This analysis reveals a densely connected structure for the fMRI, in comparison to the rewiring null model, characterized by the presence of many cliques (motif 20) and other dense configurations (motif 15 and 11) that promote highly efficient coordination between brain regions and thus high local connectivity [65], combined with an absence of sparser motifs such as $path$ (motif 1), $star$ like and $cycle$ motifs, associated to extended pathways of information transfer [65]. These results were in accordance with a previous study characterizing functional networks using 4-node subgraphs [14]. In opposition, the EEG functional networks are mainly described by less densely connected motifs, suggesting that the topology captured by this imaging technique is sparser and, therefore, less clustered than for the fMRI, which in line with the community analysis results. Nonetheless, it was found that for higher frequency bands the local structure was closer to its BOLD counterpart, selecting cliques as the most over-represented motifs. This might result from higher frequency oscillations having a tendency to be more localized, in opposition to lower frequency ones [27]. Furthermore, it is worth noting that both theta and, particularly, delta bands capture $cycle$ like motifs (motif 21) at a much higher frequency than other bands and even more than other more densely connected motifs, pointing out for a specific and interesting local topology captured by the two. From this, it is possible to conclude that the two modalities capture a functional connectivity with different levels of local clustering, equivalently to what was observed on a global level. Additionally, some motifs seem to be exclusive to each modality.

Table 7: Most commonly selected over- and under-represented motifs with 5 nodes, for each position in the top (highest and lowest significance with respect to the rewiring null model, respectively), ordered by percentage of time points, for both fMRI and EEG frequency bands, combining all subjects.

Top	1	2	3	4	5
Over-represented					
fMRI	20	15	11	8	9,12
EEG delta	21,19,15	18,19	18,19,16	16	11,16,-
EEG theta	21,19	18	19,18,16	16,11	11,16,-
EEG alpha	19,21,15	18,19,15	16,19,18	16	11,15,-
EEG beta	15,19,20	15,18	11,19	16,11	9,-
EEG gamma	20,15	15	11	8,11,19	8,16,19,-
Under-represented					
fMRI	1	4	3	-	-
EEG delta	1	2	17	13,4	6,-
EEG theta	1	2	17	13,4	-
EEG alpha	1	2	17	13	-
EEG beta	1	2	17	13	-
EEG gamma	1	2	17	13	10,-

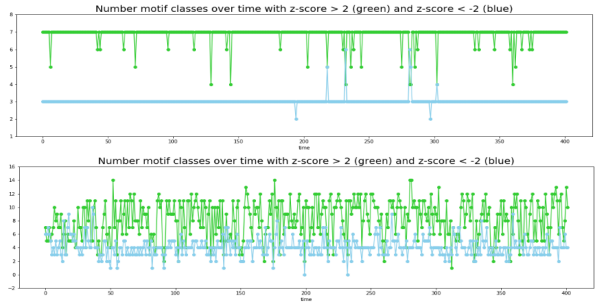

Figure 8: Temporal variation of number of motif classes over- (in green) and under-represented (in blue) with respect to the rewiring null model, for subgraphs with 5 nodes, for fMRI and EEG beta, respectively.

Regarding the temporal variation of the number of motifs retrieved, first, it is possible to observe that, for the fMRI, all time points capture over- and under-represented motifs, with respect to the rewiring null model. Suggesting that these functional networks are locally optimized for efficient communication at all times. That is not the case for the EEG, with some time points where the networks present a local organization closer to this null model, alternating with others further away. This fluctuation across time might arise from EEG's higher temporal resolution, in comparison to the fMRI, but might also be due to this imaging technique's increased susceptibility to noise. Moreover, the number of motif classes over-represented is overall higher than the under-represented ones, translating into a rich repertoire of motifs characterizing the local structure of both modalities functional networks.

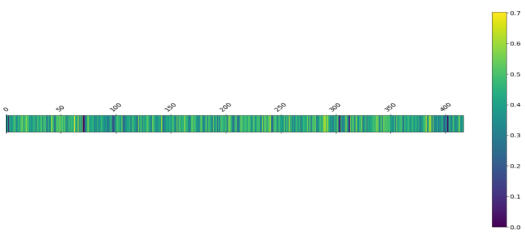

Figure 9: Cosine similarity array, resulting from the comparison of the network fingerprints between fMRI and EEG gamma for all time points, with respect to the rewiring null model, for subgraphs with 5 nodes, for subject 6.

Despite these differences in local structure for fMRI and EEG, some similar over- and under-represented motifs were captured for the two modalities, independently of the frequency band, as both capture patterns that favor efficient information transfer locally and show a reduced presence of sparser ones. As such, some moderate similarity was found with $r_\delta = 0.375$, $r_\theta = 0.352$, $r_\alpha = 0.370$, $r_\beta = 0.380$ and $r_\gamma = 0.415$ corresponding to the average cosine similarity values (excluding time points with no motif retrieved), for each frequency band.

5.5.2 Motif Analysis with Spatial Null Model

The overall results of the motif analysis of fMRI and EEG functional networks, with respect to the spatial null model are reported hereafter, to discriminate the influence of space in the local structure captured, considering again only 5 node subgraphs. Table 8 summarizes the most recurrently over- and under-represented motifs order according to the percentage of time points they appear in. Figure 10 illustrates the temporal variation of the number of motifs over- and under-expressed in these functional networks. Figure 11 shows the correlation between fMRI and EEG network fingerprints over time.

Table 8: Most commonly selected over- and under-represented motifs with 5 nodes, for each position in the top (highest and lowest significance with respect to the degree constrained spatial null model, respectively), ordered by percentage of time points, for both fMRI and EEG frequency bands, combining all subjects. The symbol - is used when no motif class is present, meaning that for most time points no significant subgraph was selected.

Top	1	2	3	4	5
Over-represented					
fMRI	-	-	-	-	-
EEG delta	21,19,-	18,-	-	-	-
EEG theta	21,-	-	-	-	-
EEG alpha	-	-	-	-	-
EEG beta	20,-	-	-	-	-
EEG gamma	20,-	15,-	17,-	-	-
Under-represented					
fMRI	3	8	4	1	5
EEG delta	-	-	-	-	-
EEG theta	-	-	-	-	-
EEG alpha	1,-	3,1,-	3,-	4,-	4,-
EEG beta	1,-	-	-	-	-
EEG gamma	-	-	-	-	-

From these results, one can immediately notice a clear distinction between the fMRI and EEG relatively to the proximity effects in the local structure. For the fMRI, no over-represented motif was obtained for the majority of time points, implying that the densely connected local structure observed previously is explained by the spatial constraints. However, it was retrieved under-represented motifs, meaning that the sparsity of these networks is substantially lower than expected by the spatial embedding. The lack of these sparser configurations translates in a preference of the fMRI networks in having superposition between the densely connected clusters, composed by cliques, instead of having loosely connected groups of brain regions. In fact, several studies have suggested that the brain networks can also be overlapping, that is,

to some extent, brain regions may belong to several modules [66–68]. For the EEG, the local structure seems to deviate positively from the spatial embedding, appearing slightly more densely connected for some time points and even presenting the same unexpected motifs for the lower frequency bands, namely motif 21 as reported in section 5.5.1. This further points out for the relevance of this motif in the topology captured by delta band. Moreover, the alpha band captured an interesting structure as it includes both over- and under-represented motif, for a substantial portion of time points, unlike any other frequency band. Therefore, contrary to what was found with respect to the rewiring null model, the densely connected structure does not increase with frequency. Instead, it is observed a high heterogeneity between frequency bands, each capturing a different topology deviating from the spatial constraints.

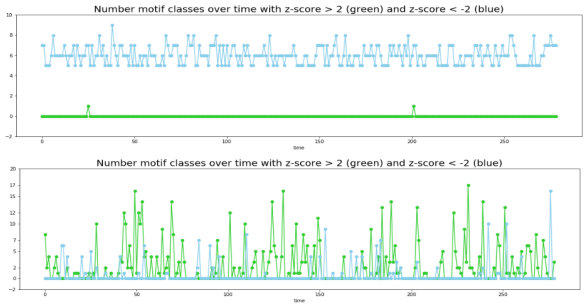

Figure 10: Temporal variation of number of motif classes over- (in green) and under-represented (in blue) with respect to the degree constrained spatial null model, for subgraphs with 5 nodes, for fMRI and EEG beta, respectively.

The temporal variation of number of motifs classes present in the networks further corroborates these findings. Furthermore, it is possible to notice that fMRI functional networks report under-represented motifs for all time points, with very little oscillations over time, while only a portion of the time points deviates from the spatial null model for the EEG. These results are in accordance to the ones obtained in the community analysis.

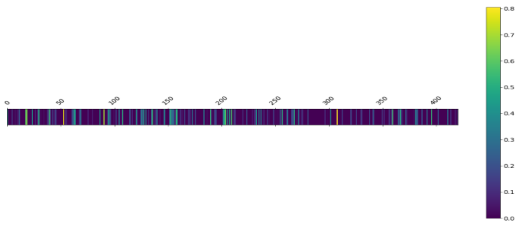

Figure 11: Cosine similarity array, resulting from the comparison of the network fingerprints between fMRI and EEG delta for all time points, with respect to the degree constrained spatial null model, for subgraphs with 5 nodes, for subject 9.

With clear differences between the two modalities, even further evidenced with this analysis, the correlation between their local structure deviating from the spatial null model was reduced, with only a few time points revealing some level of similarity: $r_\delta = 0.112$, $r_\theta = 0.049$, $r_\alpha = 0.236$, $r_\beta = 0.135$ and $r_\gamma = 0.131$ corresponding to the average cosine similarity values, for each frequency band. However, the alpha band was the exception, still showing a relevant correlation with the fMRI motif profile, consistent over time, particularly for 5 node subgraphs.

6. Conclusions and future prospects

From this work it is possible to draw several conclusions. First of all, the fMRI and EEG functional connectivity seem to capture different information on both global and local levels. On one hand, the fMRI networks showed more modular configuration, consistent over time, also being characterized by densely connected motifs, with the presence of many cliques and absence of sparser motifs. On the other hand, the EEG captures a less clustered topology, both on a macro- and meso-scale, with lower modularity and less densely connected subgraphs, with each frequency band capturing a slightly different structure oscillating across time. Moreover, when combining the two modalities, interesting and relevant communities were extracted, that would not be possible with each network individually. Secondly, both functional networks' organization is mostly explained by the spatial influence, giving preference to close connections. Nevertheless, interesting communities and densely connected patterns were still obtained beyond the proximity constraints, for both fMRI and EEG, in particular for the delta, alpha and gamma bands. Finally, despite the differences between the two modalities, there is a correlation between them over time, which is mostly explained by the spatial embedding. Nonetheless, when investigating these networks structure beyond the influence of space, a small correlation was still retrieved for a small portion of time points. Interestingly, this correlation was not equivalent between the two perspectives.

Therefore, it is possible to conclude that, even though fMRI and EEG functional connectomes are slightly linked, the two essentially capture different information, on a topological level. As such, combining the two modalities seems to be desirable to characterize the brain's complex activity and to distinguish different states and conditions. Furthermore, this work reinforces the importance of analyzing these functional networks choosing a null model that better mimics the brain networks organization, to retrieve the truly meaningful features arising from functional connectivity.

7. Acknowledgments

This document was written and made publicly available as an institutional academic requirement and as a part of the evaluation of the MSc thesis Information Systems and Computer Engineering of the author at Instituto Superior Técnico. The work described herein was performed at the Institute for Bioengineering and Biosciences of Instituto Superior Técnico and INESC-ID, during the period between February - December 2020, under the supervision of professor Alexandre Francisco and professor Patrícia Figueiredo.

References

[1] Martijn P. van den Heuvel and Hilleke E. Hulshoff Pol. Exploring the brain network: A review on resting-state fMRI functional connectivity. *European Neuropsychopharmacology*, 20(8):519–534, 2010.

[2] Elena A. Allen, Eswar Damaraju, Sergey M. Plis, Erik B. Erhardt, Tom Eichele, and Vince D. Calhoun. Tracking whole-brain connec-

tivity dynamics in the resting state. *Cerebral Cortex*, 24(3):663–676, 2014.

[3] Rodolfo Abreu, Alberto Leal, and Patrícia Figueiredo. Identification of epileptic brain states by dynamic functional connectivity analysis of simultaneous EEG-fMRI: a dictionary learning approach. *Scientific Reports*, 9(1):1–18, 2019.

[4] Ed Bullmore and Olaf Sporns. Complex brain networks: Graph theoretical analysis of structural and functional systems. *Nature Reviews Neuroscience*, 10(3):186–198, 2009.

[5] Maria Giulia Preti, Thomas AW Bolton, and Dimitri Van De Ville. The dynamic functional connectome: State-of-the-art and perspectives. *NeuroImage*, 160(December 2016):41–54, 2017.

[6] Jonathan S. Lewin. Functional MRI: An introduction to methods. *Journal of Magnetic Resonance Imaging*, 17(3):383–383, 2003.

[7] Giulia Mele, Carlo Cavaliere, Vincenzo Alfano, Mario Orsini, Marco Salvatore, and Marco Aiello. Simultaneous EEG-fMRI for functional neurological assessment. *Frontiers in Neurology*, 10(JUL), 2019.

[8] Qingbao Yu, Lei Wu, David A. Bridwell, Erik B. Erhardt, Yuhui Du, Hao He, Jiayu Chen, Peng Liu, Jing Sui, Godfrey Pearlson, and Vince D. Calhoun. Building an EEG-fMRI multi-modal brain graph: A concurrent EEG-fMRI study. *Frontiers in Human Neuroscience*, 10(SEP2016):1–17, 2016.

[9] Lucie Bréchet, Denis Brunet, Gwénaël Birot, Rolf Gruetter, Christoph M. Michel, and João Jorge. Capturing the spatiotemporal dynamics of self-generated, task-initiated thoughts with EEG and fMRI. *NeuroImage*, 2019.

[10] David T. Jones, Prashanthi Vemuri, Matthew C. Murphy, Jeffrey L. Gunter, Matthew L. Senjem, Mary M. Machulda, Scott A. Przybelski, Brian E. Gregg, Kejal Kantarci, David S. Knopman, Bradley F. Boeve, Ronald C. Petersen, and Clifford R. Jack. Non-stationarity in the "resting brain's" modular architecture. *PLoS ONE*, 2012.

[11] Richard F. Betzel, Makoto Fukushima, Ye He, Xi Nian Zuo, and Olaf Sporns. Dynamic fluctuations coincide with periods of high and low modularity in resting-state functional brain networks. *NeuroImage*, 2016.

[12] Makoto Fukushima and Olaf Sporns. Comparison of fluctuations in global network topology of modeled and empirical brain functional connectivity. *PLoS Computational Biology*, 2018.

[13] Olaf Sporns and Rolf Kötter. Motifs in Brain Networks. *PLoS Biology*, 2004.

[14] Sarah E. Morgan, Sophie Achard, Maite Termenon, Edward T. Bullmore, and Petra E. Vértes. Low-dimensional morphospace of topological motifs in human fMRI brain networks. *Network Neuroscience*, 2018.

[15] James A. Roberts, Alistair Perry, Anton R. Lord, Gloria Roberts, Philip B. Mitchell, Robert E. Smith, Fernando Calamante, and Michael Breakspear. The contribution of geometry to the human connectome. *NeuroImage*, 2016.

[16] David Samu, Anil K. Seth, and Thomas Nowotny. Influence of Wiring Cost on the Large-Scale Architecture of Human Cortical Connectivity. *PLoS Computational Biology*, 2014.

[17] Farnaz Zamani Esfahlani, Maxwell A. Bertolero, Danielle S. Bassett, and Richard F. Betzel. Space-independent community and hub structure of functional brain networks. *NeuroImage*, 2020.

[18] Vincent D. Blondel, Jean Loup Guillaume, Renaud Lambiotte, and Etienne Lefebvre. Fast unfolding of communities in large networks. *Journal of Statistical Mechanics: Theory and Experiment*, 2008.

[19] Peter J. Mucha, Thomas Richardson, Kevin Macon, Mason A. Porter, and Jukka Pekka Onnela. Community structure in time-dependent, multiscale, and multiplex networks. *Science*, 2010.

[20] Pedro Ribeiro. *Efficient and scalable algorithms for network motifs discovery*. PhD thesis, Faculdade Ciências da Universidade do Porto, Porto, Portugal, 2011.

[21] Remy Cazabet, Pierre Borgnat, and Pablo Jensen. Enhancing space-aware community detection using degree constrained spatial null model. In *Springer Proceedings in Complexity*. 2017.

[22] Russell A. Poldrack, Thomas Nichols, and Jeanette Mumford. *Handbook of Functional MRI Data Analysis*. 2011.

[23] 2013 John R.Giudicessi, BA.Michael J.Ackerman. Assessing Functional Connectivity in the Human Brain by FMRI. *Bone*, 23(1):1–7, 2008.

[24] Enrico Glerean, Juha Salmi, Juha M. Lahnakoski, Iiro P. Jääskeläinen, and Mikko Sams. Functional Magnetic Resonance Imaging Phase Synchronization as a Measure of Dynamic Functional Connectivity. *Brain Connectivity*, 2(2):91–101, 2012.

[25] Joana Cabral, Diego Vidaurre, Paulo Marques, Ricardo Magalhães, Pedro Silva Moreira, José Miguel Soares, Gustavo Deco, Nuno Sousa, and Morten L. Kringelbach. Cognitive performance in healthy older adults relates to spontaneous switching between states of functional connectivity during rest. *Scientific Reports*, 7(1), 2017.

[26] Gui XUE, Chuansheng CHEN, Zhong-Lin LU, and Qi DONG. Brain Imaging Techniques and Their Applications in Decision-Making Research. *Acta Psychologica Sinica*, 42(1):120–137, 2010.

[27] Fernando Lopes da Silva. EEG and MEG: Relevance to neuroscience, 2013.

[28] André M. Bastos and Jan Mathijs Schoffelen. A tutorial review of functional connectivity analysis methods and their interpretational pitfalls. *Frontiers in Systems Neuroscience*, 9(JAN2016):1–23, 2016.

[29] Jean Philippe Lachaux, Antoine Lutz, David Rudrauf, Diego Cosmelli, Michel Le Van Quyen, Jacques Martinerie, and Francisco Varela. Estimating the time-course of coherence between single-trial brain signals: An introduction to wavelet coherence, 2002.

[30] Keyvan Mahjoory, Vadim V. Nikulin, Loïc Botrel, Klaus Linkenkaer-Hansen, Marco M. Fato, and Stefan Haufe. Consistency of EEG source localization and connectivity estimates. *NeuroImage*, 152(March):590–601, 2017.

[31] Mahmoud Hassan and Fabrice Wendling. Electroencephalography Source Connectivity: Aiming for High Resolution of Brain Networks in Time and Space. *IEEE Signal Processing Magazine*, 35(3):81–96, 2018.

[32] Guido Nolte, Ou Bai, Lewis Wheaton, Zoltan Mari, Sherry Vorbach, and Mark Hallett. Identifying true brain interaction from EEG data using the imaginary part of coherency. *Clinical Neurophysiology*, 115(10):2292–2307, 2004.

[33] A. Kabbara, W. El Falou, M. Khalil, F. Wendling, and M. Hassan. The dynamic functional core network of the human brain at rest. *Scientific reports*, 7(1):2936, 2017.

[34] Margherita Lai, Matteo Demuru, Arjan Hillebrand, and Matteo Fraschini. A comparison between scalp- and source-reconstructed EEG networks. *Scientific Reports*, 8(1):1–8, 2018.

[35] Rodolfo Abreu, Alberto Leal, and Patrícia Figueiredo. EEG-informed fMRI: A review of data analysis methods. *Frontiers in Human Neuroscience*, 12(February):1–23, 2018.

[36] M. J. Rosa, J. Daunizeau, and K. J. Friston. EEG-fMRI integration: A critical review of biophysical modeling and data analysis approaches. *Journal of Integrative Neuroscience*, 9(4):453–476, 2010.

[37] Edward T Bullmore. *Fundamentals of Brain Network Analysis Andrew Zalesky*. 2016.

[38] Sergei Maslov and Kim Sneppen. Specificity and stability in topology of protein networks. *Science*, 2002.

[39] Stavros Dimitriadis, Nikos Laskaris, Vasso Tsirka, Michael Vourkas, and Micheloyannis Sifis. An EEG Study of Brain Connectivity Dynamics at the Resting State. *Nonlinear dynamics, psychology, and life sciences*, 16:5–22, 01 2012.

[40] Raphaël Liégeois, Erik Ziegler, Christophe Phillips, Pierre Geurts, Francisco Gómez, Mohamed Ali Bahri, B. T.Thomas Yeo, Andrea Soddu, Audrey Vanhaudenhuyse, Steven Laureys, and Rodolphe Sepulchre. Cerebral functional connectivity periodically (de)synchronizes with anatomical constraints. *Brain Structure and Function*, 2016.

[41] Marcus Kaiser and Claus C. Hilgetag. Nonoptimal component placement, but short processing paths, due to long-distance projections in neural systems. *PLoS Computational Biology*, 2006.

[42] André Couto Meira. Subgraph patterns in multiplex networks. Master's thesis, Faculdade Ciências da Universidade do Porto, Porto, Portugal, 2019.

[43] Tarmo Nurmi et al. Construction and multilayer motif analysis of temporal fmri brain networks. Master's thesis, Aalto University, Aalto, Finland, 2019.

[44] David Oliveira Aparício. *Network Comparison and Node Ranking in Complex Networks*. PhD thesis, Faculdade Ciências da Universidade do Porto, Porto, Portugal, 2019.

[45] Pedro Ribeiro and Fernando Silva. G-Tries: A data structure for storing and finding subgraphs. *Data Mining and Knowledge Discovery*, 28(2):337–377, 2014.

[46] João Jorge, Charlotte Bouloc, Lucie Bréchet, Christoph M. Michel, and Rolf Gruetter. Investigating the variability of cardiac pulse artifacts across heartbeats in simultaneous EEG-fMRI recordings: A 7T study. *NeuroImage*, 191(February):21–35, 2019.

[47] Jonathan Wirsich, João Jorge, Giannina R Iannotti, Elhum A Shamshiri, Frédéric Grouiller, Rodolfo Abreu, François Lazeyras, Anne-Lise Giraud, Rolf Gruetter, Sepideh Sadaghiani, and Serge Vulliémoz. EEG and fMRI connectomes are reliably related: a simultaneous EEG-fMRI study from 1.5T to 7T. *bioRxiv*, 2020.

[48] Rahul S. Desikan, Florent Ségonne, Bruce Fischl, Brian T. Quinn, Bradford C. Dickerson, Deborah Blacker, Randy L. Buckner, Anders M. Dale, R. Paul Maguire, Bradley T. Hyman, Marilyn S. Albert, and Ronald J. Killiany. An automated labeling system for subdividing the human cerebral cortex on MRI scans into gyral based regions of interest. *NeuroImage*, 2006.

[49] Sylvain Baillet, John C. Mosher, and Richard M. Leahy. Electromagnetic brain mapping. *IEEE Signal Processing Magazine*, 2001.

[50] Richard F. Betzel, Lisa Byrge, Farnaz Zamani Esfahlani, and Daniel P. Kennedy. Temporal fluctuations in the brain's modular architecture during movie-watching. *NeuroImage*, 2020.

[51] Danielle S. Bassett and Jennifer Stiso. Spatial brain networks. *Comptes Rendus Physique*, 19(4):253–264, May 2018.

[52] Fani Deligianni, Maria Centeno, David W. Carmichael, and Jonathan D. Clayden. Relating resting-state fMRI and EEG whole-brain connectomes across frequency bands. *Frontiers in Neuroscience*, 2014.

[53] Jonathan Wirsich, Enrico Amico, Anne Lise Giraud, Joaquín Goñi, and Sepideh Sadaghiani. Multi-timescale hybrid components of the functional brain connectome: A bimodal EEG-fMRI decomposition, 2019.

[54] Amir Joudaki, Niloufar Salehi, Mahdi Jalili, and Maria G. Knyazeva. EEG-based functional brain networks: does the network size matter? *PloS one*, 2012.

[55] Manuela Petti, Jlenia Toppi, Fabio Babiloni, Febo Cincotti, Donatella Mattia, and Laura Astolfi. EEG Resting-State Brain Topological Reorganization as a Function of Age. *Computational Intelligence and Neuroscience*, 2016.

[56] M. G. Puxeddu, M. Petti, F. Pichiorri, F. Cincotti, D. Mattia, and L. Astolfi. Community detection: Comparison among clustering algorithms and application to EEG-based brain networks. In *Proceedings of the Annual International Conference of the IEEE Engineering in Medicine and Biology Society, EMBS*, 2017.

[57] Amanda K. Robinson, Praveen Venkatesh, Matthew J. Boring, Michael J. Tarr, Pulkit Grover, and Marlene Behrmann. Very high density EEG elucidates spatiotemporal aspects of early visual processing. *Scientific Reports*, 2017.

[58] Anna Custo, Dimitri Van De Ville, William M. Wells, Miralena I. Tomescu, Denis Brunet, and Christoph M. Michel. Electroencephalographic Resting-State Networks: Source Localization of Microstates. *Brain Connectivity*, 2017.

[59] Jonathan Wirsich, Anne Lise Giraud, and Sepideh Sadaghiani. Concurrent EEG- and fMRI-derived functional connectomes exhibit linked dynamics, 2018.

[60] Rodolfo Abreu, João Jorge, Alberto Leal, Thomas Koenig, and Patrícia Figueiredo. EEG Microstates Predict Concurrent fMRI Dynamic Functional Connectivity States. *Brain Topography*, 2020.

[61] Maximilian Nentwich, Lei Ai, Jens Madsen, Qawi K. Telesford, Stefan Haufe, Michael P. Milham, and Lucas C. Parra. Functional connectivity of EEG is subject-specific, associated with phenotype, and different from fMRI. *NeuroImage*, 2020.

[62] Andrei Kurgansky. Functional organization of the human brain in the resting state. *Neuroscience and Behavioral Physiology*, 49, 11 2019.

[63] Jonathan Wirsich, Ben Ridley, Pierre Besson, Viktor Jirsa, Christian Bénar, Jean Philippe Ranjeva, and Maxime Guye. Complementary contributions of concurrent EEG and fMRI connectivity for predicting structural connectivity. *NeuroImage*, 2017.

[64] Javier Omar Garcia, Arian Ashourvan, Steven M. Thurman, Ramesh Srinivasan, Danielle S. Bassett, and Jean M. Vettel. Reconfigurations within resonating communities of brain regions following tms reveal different scales of processing. *Network Neuroscience*, 2020.

[65] Ann E. Sizemore, Chad Giusti, Ari Kahn, Jean M. Vettel, Richard F. Betzel, and Danielle S. Bassett. Cliques and cavities in the human connectome. *Journal of Computational Neuroscience*, 2018.

[66] Luiz Pessoa. Understanding brain networks and brain organization, 2014.

[67] B. T.Thomas Yeo, Fenna M. Krienen, Michael W.L. Chee, and Randy L. Buckner. Estimates of segregation and overlap of functional connectivity networks in the human cerebral cortex. *NeuroImage*, 2014.

[68] Mahshid Najafi, Brenton W. McMenamin, Jonathan Z. Simon, and Luiz Pessoa. Overlapping communities reveal rich structure in large-scale brain networks during rest and task conditions. *NeuroImage*, 2016.